Journal of Biomedical Optics

SPIEDigitalLibrary.org/jbo

# Ion-induced stacking of photosensitizer molecules can remarkably affect the luminescence detection of singlet oxygen in *Candida albicans* cells

Ariane Felgenträger
Fernanda Pereira Gonzales
Tim Maisch
Wolfgang Bäumler

SPIE

# Ion-induced stacking of photosensitizer molecules can remarkably affect the luminescence detection of singlet oxygen in *Candida albicans* cells

**Ariane Felgenträger, Fernanda Pereira Gonzales, Tim Maisch, and Wolfgang Bäumler**
Regensburg University Hospital, Department of Dermatology, 93053 Regensburg, Germany

**Abstract.** Singlet oxygen ($^1O_2$) is an important reactive intermediate in photodynamic reactions, particularly in antimicrobial PDT (aPDT). The detection of $^1O_2$ luminescence is frequently used to elucidate the role of $^1O_2$ in various environments, particularly in microorganisms and human cells. When incubating the fungus, *Candida albicans*, with porphyrins XF73 (5,15-bis-[4-(3-Trimethylammonio-propyloxy)-phenyl]-porphyrin) or TMPyP (5,10,15,20-Tetrakis(1-methyl-4-pyridinio)-porphyrin tetra(p-toluenesulfonate)), the $^1O_2$ luminescence signals were excellent for TMPyP. In case of XF73, the signals showed strange rise and decay times. Thus, $^1O_2$ generation of XF73 was investigated and compared with TMPyP. Absorption spectroscopy of XF73 showed a change in absorption cross section when there was a change in the concentration from $1 \times 10^{-6}$ M to $1 \times 10^{-3}$ M indicating an aggregation process. The addition of phosphate buffered saline (PBS) substantially changed $^1O_2$ luminescence in XF73 solution. Detailed experiments provided evidence that the PBS constituents NaCl and KCl caused the change of $^1O_2$ luminescence. The results also indicate that $Cl^-$ ions may cause aggregation of XF73 molecules, which in turn enhances self-quenching of $^1O_2$ via photosensitizer molecules. These results show that some ions, e.g., those present in cells *in vitro* or added by PBS, can considerably affect the detection and the interpretation of time-resolved luminescence signals of $^1O_2$, particularly in *in vitro* and *in vivo*. These effects should be considered for any other photosensitizer used in photodynamic processes.  [DOI: 10.1117/1.JBO.18.4.045002]

Keywords: porphyrin; photodynamic; singlet oxygen; luminescence; aggregation.

Paper 12512RR received Aug. 10, 2012; revised manuscript received Feb. 7, 2013; accepted for publication Mar. 14, 2013; published online Apr. 3, 2013.

## 1 Introduction

The fast development of multiresistant patterns against antibiotics of many species of bacteria has led to novel antibacterial strategies like the antibacterial photodynamic therapy (aPDT).[1,2] A lot of work has been done to develop molecular structures and their derivatives that are able to generate reactive oxygen species (ROS), which are the active agents for killing microorganisms.[3–7] The search for photosensitizers (PSs) for aPDT has caused the synthesis of various porphyrin molecules, which have been investigated regarding their photophysics and antimicrobial activity.[4,8,9] Naturally occurring porphyrins can be found endogenously, e.g., the protoporphyrin IX that is in the prosthetic group of the hemoglobin or the chlorophylls based on the chlorine structure. Some endogenous porphyrins in bacteria are used to treat acne, where *Propionibacterium acnes* is a causative of the inflammatory processes.[10] The porphyrin TMPyP has been frequently used for cell staining in order to investigate generation and decay of $^1O_2$.[11–13]

Different PSs are considered to localize in different compartments or regions in the eukaryotic or prokaryotic cell due to their number of positive charges and structure of the side chain. In order to determine the subcellular localization of PS and hence the site of $^1O_2$ generation, fluorescence microscopy is applied by exciting the respective PSs. Since the resolution of light microscopy is limited, this procedure should fail with small bacteria and fungus cells with a diameter of about 1 $\mu$m. The direct measurement of $^1O_2$ luminescence at 1270 nm might be an alternative candidate to elucidate the cellular action of $^1O_2$ because the rise and decay time of $^1O_2$ luminescence depend critically on its adjacency.[14,15] In addition, singlet oxygen luminescence can provide information about the photodynamic process in bacteria during irradiation.

XF73 is a newly synthesized porphyrin molecule that already showed a high potential in antimicrobial PDT against gram-negative and gram-positive bacteria.[16,17] However, principal data are lacking regarding its use in $^1O_2$ detection *in vitro*. Thus, it is the goal of the present study to investigate the photophysical properties of XF73 and its potential to monitor photodynamic action in microorganisms. Exemplarily $^1O_2$ luminescence detection was analyzed *in vitro* in *Candida albicans* cells. The well-known TMPyP was used for reference experiments.

## 2 Material and Methods

### 2.1 Chemicals

The cationic diporphyrin-based 5,15-bis-[4-(3-Trimethylammonio-propyloxy)-phenyl]-porphyrin (also referred to herein as XF73) with a molar mass of $M = 765.81$ g/mol, including the counter ion, was synthesized by Xiangdong Feng (Solvias Company,

Address all correspondence to: Ariane Felgenträger, Regensburg University Hospital, Department of Dermatology, Franz-Josef-Strauss-Allee 11, 93053 Regensburg, Germany. Tel: 0049-941-944-9650; Fax: 0049-941-944-8943; E-mail: ariane.felgentraeger@klinik.uni-regensburg.de

Basel, Switzerland) and kindly provided by Destiny Pharma Ltd. (Brighton, United Kingdom).

The 5,10,15,20-Tetrakis(1-methyl-4-pyridinio)-porphyrin tetra(p-toluenesulfonate) (also referred to herein as TMPyP) with a molar mass of $M = 1363.63$ g/mol, purity 97%, $NaN_3$ sodium azide, Mannitol, NaCl, KCl, $Na_2HPO_4$, $KH_2PO_4$, and $D_2O$ have been purchased by Sigma Aldrich (Taufkirchen, Germany), and were used as received. The photosensitizers (PSs) were dissolved in bi-distilled water at a stock concentration of 1 mM and stored at 4°C until use. Figure 1(a) shows the chemical structure of XF73 and TMPyP.

Phosphate-buffered saline (PBS; PAA Laboratories GmbH, Pasching, Austria) at pH 7.4 has been used for aggregation experiments and contains NaCl (0.14 M), KCl ($2.7 \times 10^{-3}$ M), $Na_2HPO_4$ ($1.0 \times 10^{-2}$ M), and $KH_2PO_4$ ($1.8 \times 10^{-3}$ M). For the NMR spectroscopy, a parent solution of the PSs dissolved in $D_2O$ was made and a PBS solution for dilution containing $D_2O$ has been prepared by adding NaCl, KCl, $Na_2HPO_4$, and $KH_2PO_4$ with the accordant concentrations.

## 2.2 *Absorption Spectrum*

Absorption spectra were recorded at room temperature with a spectrophotometer (DU640, Beckman Instruments GmbH, Munich, Germany) in a concentration range of $1 \times 10^{-6}$ M to $2 \times 10^{-3}$ M. The percentaged transmission has been measured and the absorption cross-section $\sigma(\mathrm{cm}^2)$ was calculated according to Eq. (1):

$$\sigma = -\frac{\ln(T/100)}{c \cdot l \cdot N_A}, \tag{1}$$

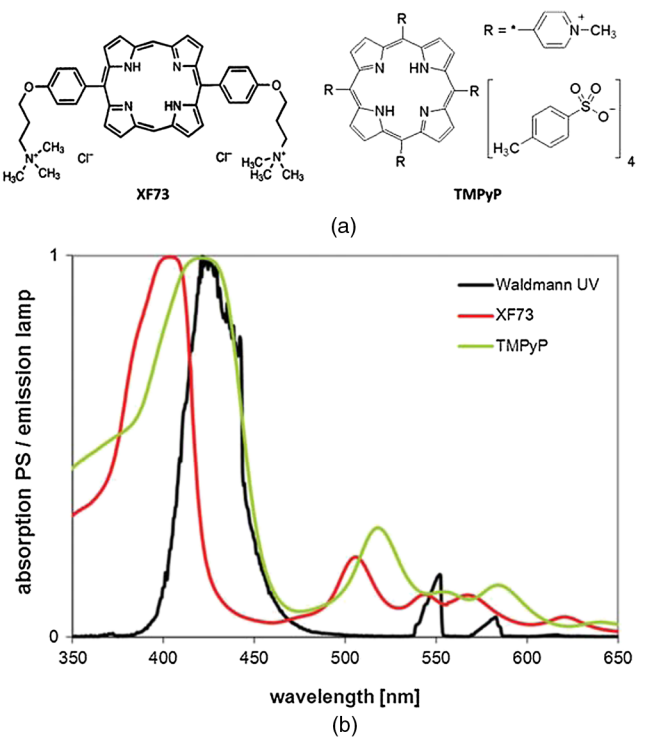


**Fig. 1** (a) Chemical structures of the porphyrins XF73 and TMPyP. (b) Normalized emission spectrum of the Waldmann-UV236 lamp. Absorption spectrum of XF73 and TMPyP with a concentration of $10^{-5}$ M each.

where $c$ the concentration of PS, l the length of light path through the solution, $T$ the transmission in percentage, and $N_A$ the Avogadro constant.

## 2.3 *Photostability*

The PSs were irradiated with an incoherent broadband lamp (UV236; emission $\lambda = 380$ to 480 nm) provided by Waldmann Medizintechnik (Villingen-Schwenningen, Germany). The maximal light intensity was 15.2 mW cm$^{-2}$ at the level of the irradiated samples. The samples were irradiated for either 15 min (13.7 J cm$^{-2}$) or 60 min (54.8 J cm$^{-2}$). The emitted spectrum of the light source was recorded with a spectrometer (270 M, Jobin Yvon, Longjumeau, France) with 300 grid lines/mm and a spectral resolution of approximately 0.4 nm [Fig. 1(b)]. The detection range was 350 to 650 nm. The recorded spectral data were corrected regarding the spectral sensitivity of the spectrometer. The emission spectrum of the Waldmann UV lamp was normalized to its maximum between 400 and 450 nm.

## 2.4 *Cell Experiments*

The *C. albicans* strain ATCC-MYA-273 was used for the experiments. The planktonic cells of *C. albicans* were diluted to a number of $10^6$. For the incubation of *C. albicans*, the PSs stock solution has been diluted with $H_2O$. The cells were incubated with a PS concentration of $10^{-4}$ M in the dark for 15 min in $H_2O$ plus 50% PBS in falcons at slow rotation. The cells were rinsed twice with PBS to remove the not included or nonadherent PSs and afterward dissolved in pure $H_2O$. For the singlet oxygen luminescence experiments, the planktonic cells were excited with a frequency doubled Nd:YAG-Laser (PhotonEnergy, Ottensoos, Germany).

## 2.5 *Fluorescence Spectrophotometer*

The localization of XF73 in *C. albicans* was examined by fluorescence microscopy (Zeiss Vario-AxioTech, Goettingen, Germany) with an appropriate dual-band filter set for excitation and emission (Omega Optical, Brattleboro, Vermont) and a 63× magnification. Planktonic *C. albicans* were incubated 2 h with $10^{-4}$ M XF73 in PBS and were rinsed twice with PBS.

## 2.6 *Singlet Oxygen Luminescence and Quantum Yield of $^1O_2$ Formation ($\Phi_\Delta$)*

Solutions with PSs were filled in a cuvette (QS-101, Hellma Optik, Jena, Germany) and solutions of the planktonic cell suspension were investigated in acrylic cuvettes (SARSTEDT, Nümbrecht, Germany), both during magnetic stirring. The PSs were excited with a frequency doubled Nd:YAG-laser (PhotonEnergy, Ottensoos, Germany) with a wavelength $\lambda = 532$ nm, power output $P = 50$ mW, frequency of $f = 2$ kHz, and therefore, energy per pulse of $E = 2.5 \times 10^{-5}$ J. Every sample was irradiated with 40,000 pulses. The *C. albicans* planktonic cells were excited with a frequency doubled Nd:YAG-laser (PhotonEnergy, Ottensoos, Germany) with a wavelength $\lambda = 532$ nm, power output $P = 60$ mW, frequency of $f = 5$ kHz, and therefore, energy per pulse of $E = 1.2 \times 10^{-5}$ J. Every sample was irradiated with 100,000 pulses.

Direct detection as described in previous papers[18–20] was done by time resolved measurements at 1270 nm (30 nm full width half maximum filter) in near-backward direction with

respect to the exciting beam using an infrared-sensitive photomultiplier (R5509-42, Hamamatsu Photonics Deutschland GmbH, Herrsching, Germany) with using an additional 950 nm cut-off-filter. The luminescence intensity is given by

$$I(t) = \frac{C}{{t_R}^{-1} - {t_D}^{-1}} \left[ \exp\left(-\frac{t}{t_D}\right) - \exp\left(-\frac{t}{t_R}\right) \right], \quad (2)$$

where $C = [T_1]_{t=0}\, k_{T1\Delta}\, [^3O_2]$ was used to fit the singlet oxygen luminescence signal, describing the deactivation of the excited triplet state $T_1$ of the photosensitizer by oxygen in its ground state ($^3O_2$).[20] $t_R$ and $t_D$ are the rise and decay times, which is the excited triplet state decay time $\tau_{T1}$ of the photosensitizer and the decay time of singlet oxygen $\tau_\Delta$. The attribution of $\tau_{T1}$ and $\tau_\Delta$ depends on the oxygen concentration in the system; at high oxygen concentrations, usually the decay time $\tau_D$ of the signal describes the decay time of singlet oxygen $\tau_\Delta$. In order to determine the rise and decay times, the Levenberg-Marquardt-algorithm of Mathematica (Wolfram Research, Champaign) was used. The luminescence signal was spectrally resolved using interference filters in front of the photomultiplier tube at wavelengths ranging from 1150 to 1400 nm or a monochromator (Horiba, Yobin Yvon Inc., USA) from 1200 to 1350 nm at 10 nm regular steps (XF73 in pure $H_2O$). The values show the integrated luminescence signals detected at a certain wavelength and are normalized to the maximal value. A Lorentz-shaped curve has been fitted through the measurement points, with the maximum at $\lambda = 1270$ nm, referring to the maximal value in $H_2O$.

For the determination of $\Phi_\Delta$ of XF73 in $H_2O$, it is compared with the $\Phi_\Delta$ of TMPyP, which is reported in literature being 0.74[21] and $0.77 \pm 0.04$[12] in aqueous solution. Therefore, five probes of each PS of different concentrations (between 30% and 70% absorption at a wavelength of $\lambda = 532$ nm) are irradiated and the emitted $^1O_2$-photons are determined with the integral over the luminescence curve, given with the fit routine mentioned.

## 3 Results and Discussion

As a first experiment, cells of *C. albicans* were incubated with XF73 or TMPyP for 15 min using a concentration of 100 $\mu$M. The cells were washed twice, suspended in $H_2O$ solution, and subsequently excited with the laser at 532 nm. TMPyP in the cells produced a clear $^1O_2$ luminescence signal with a rise time of $t_R = (1.77 \pm 0.2)\,\mu$s and a decay time of $t_D = (6.74 \pm 0.7)\,\mu$s [Fig. 2(a)]. In contrast to that, XF73 in *C. albicans* produced completely different $^1O_2$ luminescence signals showing no or a very short rise time, whereas the signal decayed in a multiexponentially manner. When starting the fit at 2 $\mu$s, the decay time was $t_D = (5.33 \pm 0.5)\,\mu$s [Fig. 2(b)].

On one hand, XF73 molecules were possibly localized at subcellular sites, where high quencher concentrations or low oxygen concentration affected the rise and decay of $^1O_2$ luminescence. On the other hand, the photophysical properties of XF73 could have been altered after the uptake of *C. albicans* cells. It is known for many porphyrin species that PS molecules can show stacking to *J*- (edge-to-edge) and *H*-aggregates (face-to-face) under certain conditions.[22,23] Aggregation of porphyrin derivatives is influenced by concentration of inorganic salts, the polarity of the solvents, or the side chains of the porphyrins,[24–26] whereas the results are still controversially discussed. Aggregation of PSs like TMPyP should not occur for concentrations of less than $10^{-4}$ M.[27–30] An overview of the discussions related to the aggregation of TMPyP is given by Vergeldt et al., who described adsorption onto surfaces or aggregation effects due to the impurity of the solvent.[31]

Stacking of porphyrin molecules could occur at high photosensitizer concentrations or could be mediated by inorganic salts, which were particularly added with PBS to cells. Photosensitizer stacking may change the rate and rate constants for XF73 molecules and thereby affect the generation and decay of $^1O_2$, which could be detected by time resolved detection of its luminescence.

### 3.1 *Absorption Spectroscopy in Aqueous PS Solution*

Changes in the $\pi$-electron-system of porphyrin molecules can lead to the change of absorption cross-section $\sigma$ and hence may affect $^1O_2$ generation. TMPyP showed a constant absorption cross-section in the range from $10^{-6}$ to $10^{-3}$ M (data not shown). In contrast to TMPyP, the absorption spectrum of XF73 in pure $H_2O$ clearly depended on XF73 concentration. The absorption cross-section decreased with increasing XF73 concentration from $10^{-5}$ to $2 \cdot 10^{-3}$ M and the absorption maximum (Soret band) shifted to shorter wavelengths (~7 nm) [Fig. 3(a)]. Both effects indicate aggregation of XF73 molecules.

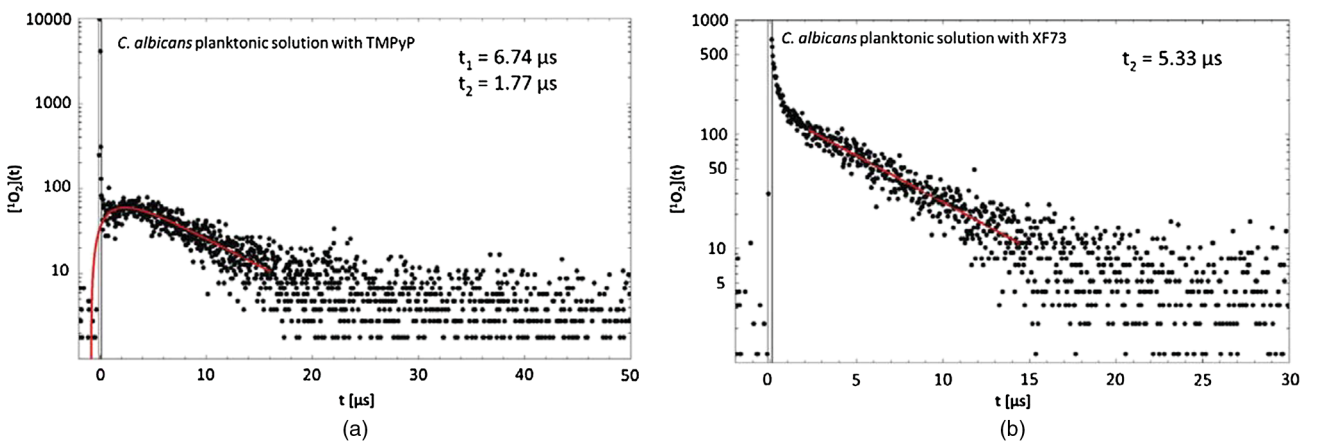


**Fig. 2** Singlet oxygen luminescence signal of planktonic solution of *C. albicans* cells incubated with $10^{-4}$ M of TMPyP (a) and XF73 (b) for 15 min in the dark. The cells were washed and are surrounded by pure $H_2O$ with a cell concentration of $10^6$ cells per mL.

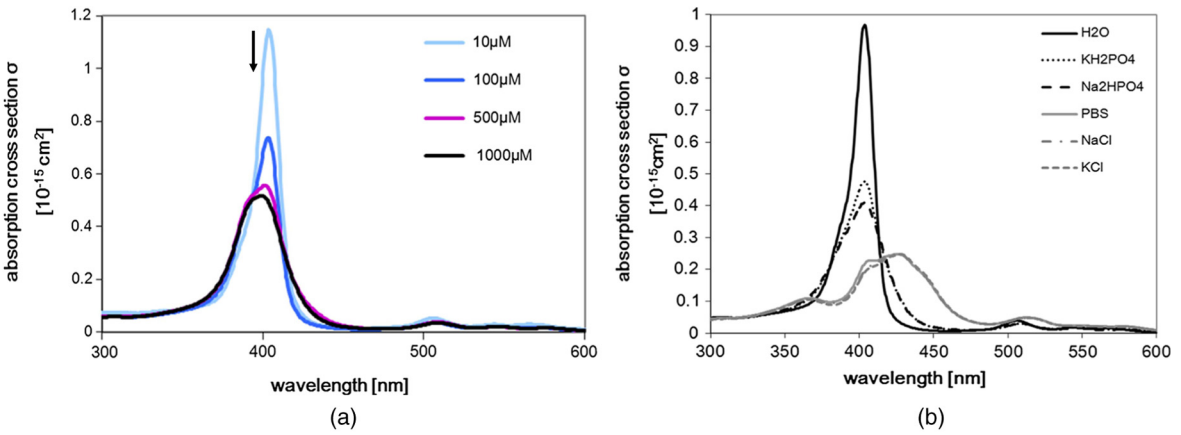


| Substance | $H_2O$ | $KH_2PO_4$ | $Na_2HPO_4$ | PBS | KCl | NaCl |
|---|---|---|---|---|---|---|
| $\lambda_{max}$ | 402 | 403.5 | 403.5 | 426 | 427.5 | 425 |
| $\sigma_{max}$ | 0.71 | 0.48 | 0.41 | 0.25 | 0.25 | 0.25 |

**Fig. 3** (a) Absorption spectrum of XF73 with increasing PS concentration. A blue-shift of the absorption maxima of 7 nm was detected when increasing the concentration from $10^{-5}$ to $10^{-3}$ M. (b) Comparison of the influence of the single components of PBS on the absorption spectrum of XF73. A PS concentration of $2 \times 10^{-5}$ M has been used and NaCl, KCl, $KH_2PO_4$, and $Na_2HPO_4$ had each a concentration of 0.1 M. The table shows the wavelengths $\lambda_{max}$ of the absorption maximum and its value $\sigma_{max}$ for each component of PBS, for PBS and $H_2O$.

### 3.2 *Absorption Spectroscopy in Aqueous XF73 Solution with PBS or PBS Constituents*

The PBS and cytosol of living cells contain various ions like $K^+$, $Na^+$, $Cl^-$, $HCO_3^-$, $Mg_2^+$, $Ca_2^+$, and $HPO_4^{2-}$. As a first approximation to cellular environment, XF73 was dissolved in PBS solution. As XF73 was not easily soluble in PBS, the maximum concentration of PBS was 50% in $H_2O$. Absorption spectra of XF73 ($2 \times 10^{-5}$ M) were recorded in pure $H_2O$, in 50% $H_2O$ plus 50% PBS, and in 100% $H_2O$ adding single constituents of PBS such as KCl, NaCl, $NaH_2PO_4$, or $KH_2PO_4$, 0.1 M each [Fig. 3(b)].

In the presence of $Na_2HPO_4$ or $KH_2PO_4$, the absorption cross-section showed no wavelength shift or new absorption maxima within given experimental accuracy (±2 nm) when compared with pure $H_2O$. The maximum value of absorption cross-section at (402 ± 2) nm decreased from $\sigma_{max} = 0.71 \times 10^{-15}$ cm$^2$ (pure $H_2O$) to $\sigma = 0.41 \times 10^{-15}$ cm$^2$ or $\sigma = 0.48 \times 10^{-15}$ cm$^2$ when $Na_2HPO_4$ or $KH_2PO_4$ was added, respectively.

When adding PBS, $\sigma_{max}$ decreased from $0.71 \times 10^{-15}$ cm$^2$ to $0.25 \times 10^{-15}$ cm$^2$ and shifted to longer wavelengths (red shift) of 24 ± 2 nm.

When adding NaCl or KCl to XF73 solution, $\sigma_{max}$ decreased to $0.25 \times 10^{-15}$ cm$^2$ for each. In addition, $\sigma_{max}$ shifted to the red by about 25 ± 3 nm. At the same time, the absorption spectrum showed new absorption maxima within the spectral range of the Soret band. Addition of $Cl^-$ leads to a fundamental change of the absorption spectrum including a red shift. It is suggested that $Cl^-$ affects the tetrapyrrol ring system and enhances the aggregation, which was already reported for other porphyrin structures.[32]

A visible precipitation of the solute started when using >10% PBS + $H_2O$. This effect was shown to be reversible by diluting the solution with pure $H_2O$. As a consequence of this dilution, the absorption spectrum of XF73 in PBS changed back to the absorption spectrum in pure $H_2O$ (data not shown). The precipitation does not affect the absorption measurements because the probes are directly used after being diluted and the precipitation effect needs several hours to develop. No light scattering effect in solutions was detectable by checking the absorption spectrum at shorter wavelengths.

### 3.3 *Photostability*

Also, the photostability and hence the change of absorption spectrum during irradiation may affect $^1O_2$ luminescence. Therefore, the photostability of XF73 in solution containing PBS was investigated when illuminating the samples up to 54.8 J cm$^{-2}$.

No changes in the absorption spectrum of TMPyP were noticed within irradiation time of upto 60 min (data not shown). The XF73 in $H_2O$ and in 50% PBS + $H_2O$ showed a decrease in absorption that was mainly detected in the spectral range of the Soret band (Fig. 4). Obviously, the presence of PBS,

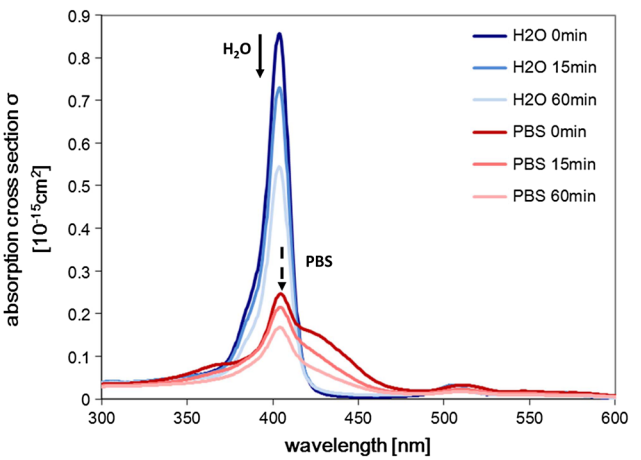


**Fig. 4** Photostability measurements with XF73 show a decrease of the absorption cross section with the time of illumination and therefore the applied energy. The light source was the Waldmann-UV236 lamp with an applied energy dose of 13.7 or 54.7 J cm$^{-2}$, respectively. XF73 with a concentration of $10^{-5}$ M has been investigated in pure $H_2O$ and in PBS (50% in $H_2O$).

i.e., its ions, can additionally reduce radiation absorption of XF73. These effects may also affect the use of XF73 when applied for photodynamic inactivation of microorganisms.

In case of $^1O_2$ experiments (see below), XF73 solutions were irradiated with 1 J of laser energy (532 nm). It is expected that $\sigma$ values do not significantly change under these experimental conditions.

### 3.4 $^1O_2$ *Luminescence Experiments without PBS*

Incubation of bacteria or human cells with XF73 and subsequent irradiation yielded effective cell killing by means of $^1O_2$ generation, which was confirmed by adding $^1O_2$ quencher $NaN_3$ that significantly reduced the cell toxicity.[16] Since detailed studies on $^1O_2$ generation of the novel porphyrin molecule XF73 were

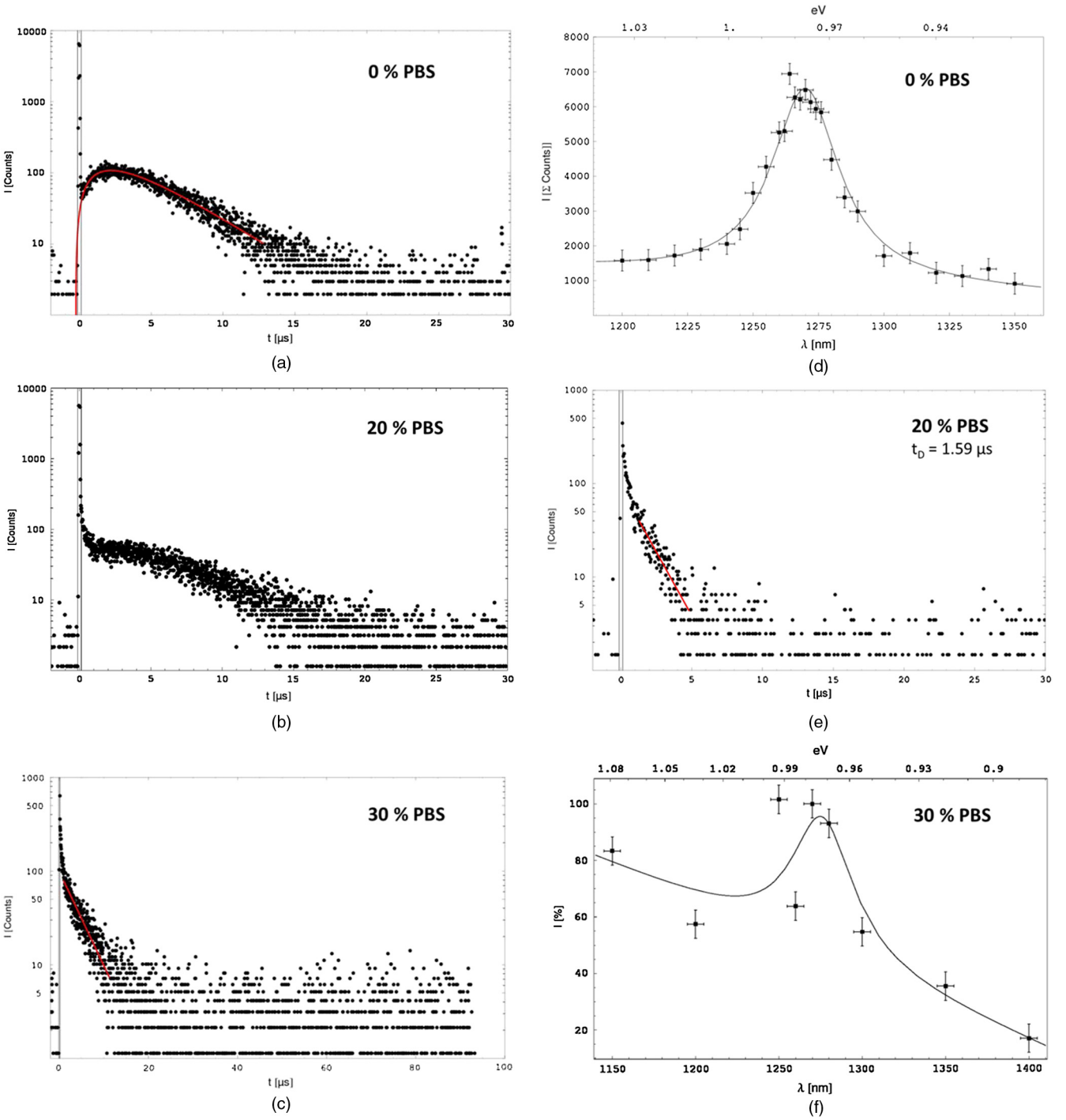


**Fig. 5** (a)–(c) $^1O_2$ luminescence signals of $[XF73] = 5 \times 10^{-5}$ M with different PBS concentrations in $H_2O$ with an oxygen concentration of $[^3O_2] = 2.7 \times 10^{-4}$ M. (d) Spectroscopically resolved $^1O_2$ luminescence signal, generated by XF73 in $H_2O$ with an oxygen concentration of $[O_2] = 2.7 \times 10^{-4}$ M. A Lorentz-shaped curve has been fitted through the measurement points. (e) $^1O_2$ luminescence generated by XF73 in $H_2O$ + 20%PBS at 1270 nm with $2 \times 10^{-3}$ M NaCl in solution. (f) Spectroscopically resolved $^1O_2$ luminescence signal, generated by XF73 in 30% PBS + $H_2O$ with an oxygen concentration of $[O_2] = 2.7 \times 10^{-4}$ M. A Lorentz-shaped curve has been fitted through the measurement points.

missing, we investigated XF73 in pure aqueous solution according to previous studies on other photosensitizers.[27]

After dissolving $[XF73] = 5 \times 10^{-5}$ M in air saturated ($[^3O_2] = 2.7 \times 10^{-4}$ M), pure $H_2O$, the rise and decay part of the time resolved signals could be assigned to the decay time $\tau_\Delta$ of $^1O_2$ and the decay time $\tau_{T1}$ of PS, respectively. Experiments yielded $\tau_{T1} = 1.6 \pm 0.2$ $\mu$s and decay time $\tau_\Delta = 3.5 \pm 0.3$ $\mu$s [Fig. 5(a)]. The decay time is in good correlation with the lifetime of $^1O_2$ in pure water.[33–35] The spectrally resolved $^1O_2$ luminescence revealed a peak at 1270 nm, which clearly confirmed the generation of $^1O_2$ [Fig. 5(d)]. The $^1O_2$ quantum yield $\Phi_\Delta$ of XF73 was determined in air saturated, pure $H_2O$, using TMPyP as reference. The $\Phi_\Delta$ values of TMPyP are 0.74[21] and $0.77 \pm 0.04$.[13] Using the previously reported technique,[21] XF73 showed a value of $\Phi_\Delta = 0.57 \pm 0.06$.

When changing the concentration of $O_2$ in the solution at a constant concentration of $[XF73] = 5 \times 10^{-5}$ M, the meaning of the rates $K_\Delta$ and $K_{T1}$ at $[^3O_2] = 1.1 \times 10^{-4}$ M changed according to the decay paths of $^1O_2$ and $T_1$ [Fig. 6(a)].[20] This change occurs at a crossing point of ${t_1}^{-1}$ and ${t_2}^{-1}$, which was about $[^3O_2] = (0.11 \pm 0.02)$ $10^{-3}$ M for XF73. By extrapolating ${t_2}^{-1}$, $K_{T1}$ ($([O_2] = 0$ M$) = 0.03$ $\mu s^{-1}$ was determined yielding a lifetime of the triplet $T_1$-state of $(33 \pm 5)$ $\mu$s in aqueous solution without oxygen quenching. The quenching rate constant $k_q$ for quenching of the excited triplet state of XF73 by oxygen is therefore $k_q = 2.3 \times 10^9$ $s^{-1}$ $M^{-1}$ resulting from the Stern-Volmer-plot in Fig. 6(a), where the oxygen concentration was varied and the triplet decay of XF73 was determined.

As a next step, XF73 concentration was varied from $[XF73] = 10^{-6}$ to $5 \times 10^{-3}$ M at $[[^3O_2] = 5.6 \times 10^{-5}$ M [Fig. 6(b)]. The value of ${t_2}^{-1}$ increased with increasing concentration that indicated a clear self-quenching effect of the excited triplet-$T_1$-state for [XF73] up to about $2 \times 10^{-4}$ M. Above this concentration, the quenching effect decreased and reached a plateau at ${t_2}^{-1} = 0.205$ $\mu s^{-1}$, which is equivalent to a decay time of the triplet-$T_1$-state of $t_{T1} = 4.9$ $\mu$s [Fig. 6(b)]. According to the absorption spectroscopy data, a stacking of XF73 molecules occurred, which is easily detectable for XF73 concentration higher than $1 \times 10^{-4}$ M [Fig. 3(a)]. Obviously, the stacking process had already led to the formation of dimers or oligomers of XF73 molecules at this concentration. Besides a different absorption cross-section, these aggregates also show different deactivation of triplet $T_1$-state as compared with XF73 monomers [Fig. 6(b)].

### 3.5 $^1O_2$ *Luminescence Experiments with PBS*

In light of the results above, $^1O_2$ luminescence signals should be affected by molecule stacking, in particular when the photosensitizer in located in *C. albicans* cells [Fig. 2(b)]. Therefore, we investigated the PBS effect on time-resolved $^1O_2$ luminescence generated by XF73 in air saturated solution at a concentration of $5 \times 10^{-5}$ M, for which stacking due to PS concentration should be still minimal [Fig. 3(a)]. The results clearly show that $^1O_2$ luminescence substantially changed with increasing PBS concentration [Fig. 5(a)–5(c)]. From 0% to 50% PBS in $H_2O$, the rising part of $^1O_2$ luminescence signal disappeared, whereas the decaying part shortened. Now, the luminescence signals at high PBS concentrations [Fig. 5(c)] were similar to those recorded for XF73 in *C. albicans* cells [Fig. 2(b)] yielding again a multiexponential decay.

When adding $^1O_2$ quencher $NaN_3$[36,37] to the 20% PBS solution up to a high concentration of $2 \times 10^{-3}$ M $NaN_3$, the $^1O_2$ luminescence signal almost disappeared. The residual signal should not originate from $^1O_2$ luminescence [see Fig. 5(e)]. The same residual signal was detected in solutions without $NaN_3$ and without oxygen (data not shown).

$^1O_2$ luminescence was also spectrally resolved for PBS 0% and 50% in $H_2O$ [Fig. 5(d) and 5(f)]. A Lorentz-shaped curve has been fitted through the measurement points and the values were normalized to the maximal value. Without PBS, the fit shows a clear maximum at 1270 nm that confirms the generated $^1O_2$.[38] At 50% PBS, the maximum at 1270 nm almost disappeared, the baseline moved for wavelengths <1270 nm, and the signal-to-noise ratio decreased, which indicates a substantial decrease of $^1O_2$ generation.

Comparable to absorption spectroscopy, the changes of time- and spectral resolved $^1O_2$ luminescence signals, induced by PBS, could be simply reversed by diluting the used solutions with $H_2O$ and hence reducing the PBS concentration. A high degree of dilution of PBS concentration yielded time- and spectrally resolved $^1O_2$ luminescence signals comparable with Fig. 5(a) and 5(d).

Scattering of photons within solution might also cause a $^1O_2$ luminescence signal equal to the one in Fig. 5(e), and might be

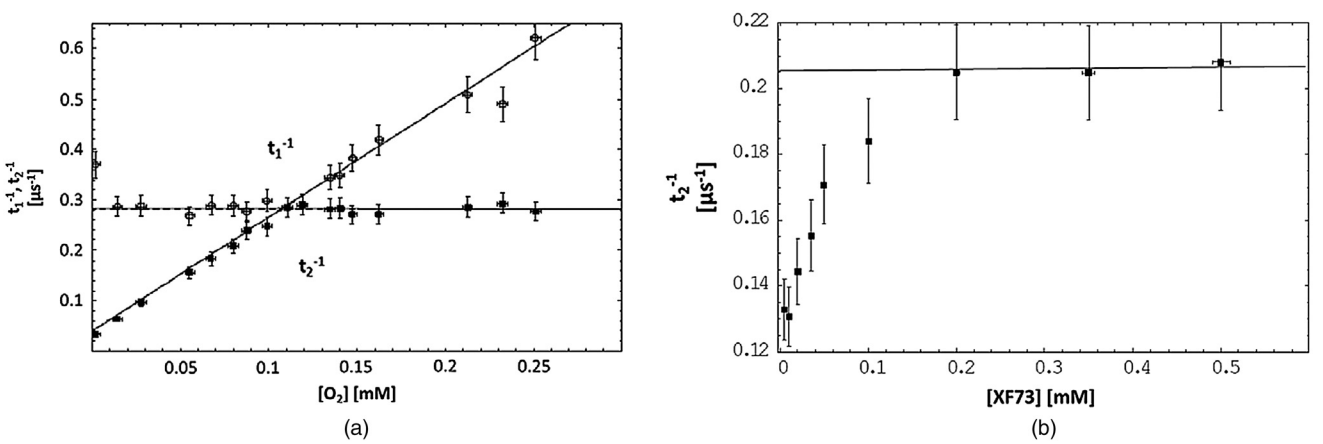


**Fig. 6** (a) Rates ${t_1}^{-1}$ and ${t_2}^{-1}$ of the time resolved $^1O_2$ signal depending on the concentration of $O_2$. The meaning of the two rates changes at the crossing point of the curves. (b) The rate ${t_2}^{-1}$ characterizes the decay time of the triplet-$T_1$-state and changes with the XF73 concentration; here the oxygen concentration is kept constant at $[^3O_2] = 5.4 \times 10^{-5}$ M.

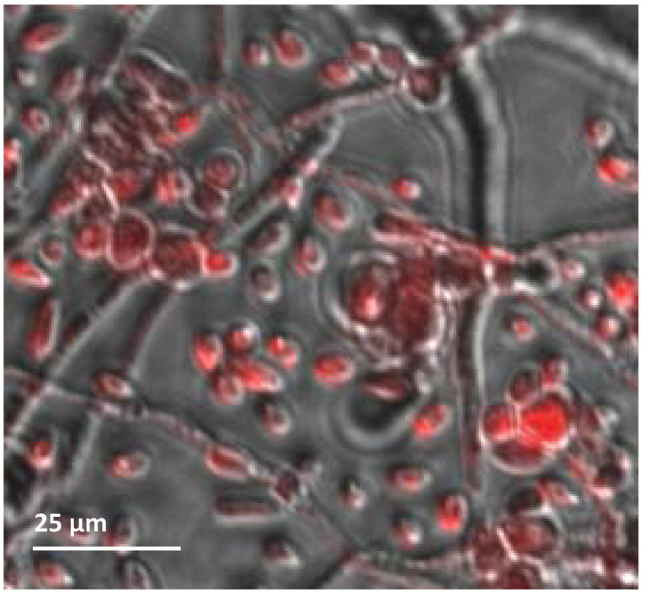


**Fig. 7** Fluorescence image of *C. albicans;* the cells were incubated 2 h with $10^{-4}$ M XF73 in PBS and rinsed twice. An attachment of XF73 to the cells can be seen.

originating from precipitation due to the stacking of the porphyrins. To exclude any scattering effects, the scattering agent $SiO_2$ was added to aqueous solutions containing $5 \times 10^{-5}$ M XF73 or TMPyP. No effect on the shape of the $^1O_2$ luminescence signal and no change of the rise and decay times were detected for both photosensitizers. Additionally there was no scattering effect visible in the absorption spectrum of XF73 in $H_2O + 50\%$ PBS.

## 4 Conclusions

The detection of singlet oxygen by its luminescence is a great tool to show the action of singlet oxygen even in cells or bacteria. In this context it is important to have a detection procedure that provides reliable data from inside such cells, in particular when knowing that cellular constituents can substantially affect singlet oxygen luminescence. The interaction of porphyrins with *C. albicans* is controversially discussed that ranges from no uptake to tight binding or even internalization.[39–43] Many porphyrins are lipophilic and hence should accumulate in cellular membranes but the high water-solubility of XF73 suggests localization in the cytoplasm as well. Fluorescence microscopy showed the overall attachment of XF73 to the cell after washing; however, the low spatial resolution of optical microscopy impedes the evaluation of the subcellular photosensitizer localization (Fig. 7). Thus, it would be of importance to gain additional insight by evaluating the $^1O_2$ luminescence data.

However, XF73 showed substantial stacking of molecules that affected light absorption as well as the generation and decay of $^1O_2$. Stacking already occurred in pure $H_2O$ along with the increase of the PS concentration. The stacking is additionally forced by the ionic pressure of $Cl^-$. Such ions are either present in cells or are usually added in cell experiments *in vitro* via PBS to protect the cells from osmosis. Therefore, it is impossible to exclude such ions when investigating photosensitizers in cell experiments.

Depending on the uptake mechanisms and the chemical structure, a PS localizes in cellular membranes or in the cytoplasm close to any cellular structures.[44,45] Cytoplasm shows a similar concentration of $Cl^-$ like PBS; therefore, it is very likely that aggregation of XF73 occurs in cells such as *C. albicans*. The time-resolved detection of the $^1O_2$ luminescence in a solution of planktonic *C. albicans* cells incubated with XF73 and surrounded by pure $H_2O$ has been done [Fig. 2(b)]. In fact, the luminescence signal is similar to the signal of XF73 generating $^1O_2$ in 30% PBS [Fig. 5(c)] showing a multiexponential decay. This signal indicates a surrounding of XF73 within *C. albicans* cells whose ionic concentration is similar to that of >30% PBS. Usually, the rise and decay times of luminescence provides information about the localization of $^1O_2$ and hence of the photosensitizer applied due to the short diffusion length of $^1O_2$ in cells. As the molecule XF73 is strongly influenced by the salts of the phosphate buffer PBS, such interpretations could be misleading at the moment. This problem may also occur for any other PS that undergoes stacking in the presence of ions such as $Cl^-$.

Despite the results with XF73, the $^1O_2$ luminescence detection in cells is a great tool to elucidate photodynamic processes. The porphyrin TMPyP showed neither stacking in the investigated range of concentration nor interference with the salts of PBS. After attached to or taken up by *C. albicans,* the generated $^1O_2$ could be easily detected by its luminescence with clear rise and decay components. The decay time of the $^1O_2$ luminescence in Fig. 2(a) of $t_D = (6.74 \pm 0.5)\,\mu s$, which is clearly longer than in pure water (3.5 $\mu$s) and can be most likely attributed to the decay time of the $T_1$-state of TMPyP. If so, a triplet state decay time of 6.74 $\mu$s suggests an oxygen concentration of its surrounding of $[O_2] = 8 \times 10^{-5}$ M, which is 30% compared with the oxygen concentration of $[O_2]_{sat} = 2.7 \times 10^{-4}$ M of air saturated water.

Nevertheless, the striking phototoxic effect of XF73 in bacteria was demonstrated.[16] *In vitro* experiments showed a substantial reduction of bacteria (~8 $\log_{10}$ steps), which were incubated very small XF73 concentrations ($10^{-8}$ M) for 5 min and subsequently irradiated with 13.7 J cm$^{-2}$. The action of $^1O_2$ was proven with the addition of the $^1O_2$ quencher $NaN_3$; however, the photodynamic effect could not be completely inhibited by the quencher. In addition, the rather small XF73 concentration in the range of 0.01 to 10 $\mu$M in those bacteria experiments could have minimized the stacking effect and therefore maximized phototoxicity by an effective singlet oxygen generation.

Aggregation effects influence also the fluorescence of a dye, which has recently been described by López-Chicón et al. with an investigation of Hypericin in different species of *Candida*.[46] The grade of aggregation depends on the surrounding and the fluorescence is low or not existent at a high PS aggregation, which occurs in $H_2O$-environment. Upon incubation of different species of *Candida* with Hypericin, one can draw a conclusion about the localization of the PS by monitoring the radiative decay, here the fluorescence that depends on the aggregation status.

Recently, with an optimized experimental setup singlet oxygen generation in *C. albicans* cells was detected by irradiating directly the Soret-band of the porphyrin TMPyP at 420 nm.[47] With irradiation of the absorption maximum, it is possible to detect singlet oxygen generation and decay at already very low photosensitizer concentrations in the range of few $\mu$M offering a concentration range where aggregation effects are expected to be low and thus the singlet oxygen generation is effective.

Since the phototoxic efficacy depends on the localization and also on the aggregation status of the photosensitizer, which is influenced by ions, further investigations and comparative

studies on the change of the singlet oxygen luminescence in different species of microorganisms should lead to better insights about the change of the decay times due to the localization.

## References


1. C. A. Hart and S. Kariuki, "Antimicrobial resistance in developing countries," *BMJ* **317**(7159), 647–650 (1998).
2. R. Wise et al., "Antimicrobial resistance. Is a major threat to public health," *BMJ* **317**(7159), 609–610 (1998).
3. M. Wainwright, "Photodynamic antimicrobial chemotherapy (PACT)," *J. Antimicrob. Chemother.* **42**(1), 13–28 (1998).
4. K. Lang, J. Mosinger, and D. M. Wagnerova, "Photophysical properties of porphyrinoid sensitizers non-covalently bound to host molecules; models for photodynamic therapy," *Coord. Chem. Rev.* **248**(3–4), 321–350 (2004).
5. M. R. Hamblin and T. Hasan, "Photodynamic therapy: a new antimicrobial approach to infectious disease?," *Photochem. Photobiol. Sci.* **3**(5), 436–450 (2004).
6. M. Niedre, M.S. Patterson, and B.C. Wilson, "Direct near-infrared luminescence detection of singlet oxygen generated by photodynamic therapy in cells *in vitro* and tissues *in vivo*," *Photochem. Photobiol.* **75**(4), 382–391 (2002).
7. G. Jori and S. B. Brown, "Photosensitized inactivation of microorganisms," *Photochem. Photobiol. Sci.* **3**(5), 403–405 (2004).
8. R. Bonnett, "Photosensitizers of the porphyrin and phthalocyanine series for photodynamic therapy," *Chem. Soc. Rev.* **24**(1), 19–33 (1995).
9. R. Bonnett and M. Berenbaum, "Porphyrins as photosensitizers," *Ciba Found. Symp.* **146**, 40–59; discussion 53–59 (1989).
10. K. Nouri and L. M. Villafradez-Diaz, "Light/laser therapy in the treatment of acne vulgaris," *J. Cosmet. Dermatol.* **4**(4), 318–320 (2005).
11. E. Feese and R. A. Ghiladi, "Highly efficient in vitro photodynamic inactivation of Mycobacterium smegmatis," *J. Antimicrob. Chemother.* **64**(4), 782–785 (2009).
12. P. K. Frederiksen et al., "Two-photon photosensitized production of singlet oxygen in water," *J. Am. Chem. Soc.* **127**(1), 255–269 (2005).
13. J. W. Snyder, J. D. Lambert, and P. R. Ogilby, "5,10,15,20-tetrakis(N-methyl-4-pyridyl)-21H,23H-porphine (TMPyP) as a sensitizer for singlet oxygen imaging in cells: characterizing the irradiation-dependent behavior of TMPyP in a single cell," *Photochem. Photobiol.* **82**(1), 177–184 (2006).
14. X. Ragas, M. Agut, and S. Nonell, "Singlet oxygen in Escherichia coli: new insights for antimicrobial photodynamic therapy," *Free. Radic. Biol. Med.* **49**(5), 770–776 (2010).
15. E. F. de Silva et al., "Irradiation- and sensitizer-dependent changes in the lifetime of intracellular singlet oxygen produced in a photosensitized process," *J. Phys. Chem. B* **116**(1), 445–461 (2012).
16. T. Maisch et al., "Photodynamic effects of novel XF porphyrin derivatives on prokaryotic and eukaryotic cells," *Antimicrob. Agents. Chemother.* **49**(4), 1542–1552 (2005).
17. F. Pereira Gonzales and T. Maisch, "XF drugs: a new family of antibacterials," *Drug News Perspect.* **23**(3), 167–174 (2010).
18. J. G. Parker and W. D. Stanbro, "Optical determination of the rates of formation and decay of O-2(1-Delta-G) in $H_2O$, $D_2O$ and other solvents," *J. Photochem.* **25**(2–4), 545–547 (1984).
19. J. Regensburger et al., "A helpful technology–the luminescence detection of singlet oxygen to investigate photodynamic inactivation of bacteria (PDIB)," *J. Biophoton.* **3**(5–6), 319–327 (2010).
20. J. Baier et al., "Theoretical and experimental analysis of the luminescence signal of singlet oxygen for different photosensitizers," *J. Photochem. Photobiol. B* **87**(3), 163–173 (2007).
21. F. Wilkinson, W. P. Helman, and A. B. Ross, "Quantum yields for the photosensitized formation of the lowest electronically excited singlet-state of molecular-oxygen in solution," *J. Phys. Chem. Ref. Data* **22**(1), 113–262 (1993).
22. F. Ricchelli, "Photophysical properties of porphyrins in biological membranes," *J. Photochem. Photobiol. B*, **29**(2–3), 109–118 (1995).
23. E. Zenkevich et al., "Photophysical and photochemical properties of potential porphyrin and chlorin photosensitizers for PDT," *J. Photochem. Photobiol. B-Biol.* **33**(2), 171–180 (1996).
24. K. M. Kadish, K. M. Smith, and R. Guilard, *The Porphyrin Handbook*, Academic Press, San Diego (2000).
25. N. C. Maiti et al., "Fluorescence dynamics of noncovalently linked porphyrin dimers and aggregates," *J. Phys. Chem.* **99**(47), 17192–17197 (1995).
26. M. Sirish and H. J. Schneider, "Supramolecular chemistry, part 93—Electrostatic interactions between positively charged porphyrins and nucleotides or amides: buffer-dependent dramatic changes of binding affinities and modes," *Chem. Commun.* **1**, 23–24 (2000).
27. R. F. Pasternack et al., "On the aggregation of meso-substituted water-soluble porphyrins," *J. Am. Chem. Soc.* **94**(13), 4511–4517 (1972).
28. K. Kano et al., "Evidence for stacking of cationic porphyrin in aqueous-solution," *Chem. Lett* **12**, 1867–1870 (1983).
29. R. L. Brookfield, H. Ellul, and A. Harriman, "Luminescence of porphyrins and metalloporphyrins. 9. Dimerization of meso-tetrakis(N-Methyl-4-Pyridyl)-porphine," *J. Photochem.* **31**(1), 97–103 (1985).
30. K. M. Kadish, B. G. Maiya, and C. Araullomcadams, "Spectroscopic characterization of meso-tetrakis(1-Methylpyridinium-4-Yl)porphyrins, [(Tmpyp)H2]4+ and [(Tmpyp)M]4+, in aqueous micellar media, where $M$ = Vo2+, Cu(Ii), and Zn(Ii)," *J. Phys. Chem.* **95**(1), 427–431 (1991).
31. F. J. Vergeldt et al., "Intramolecular interactions in the ground and excited-state of tetrakis(N-Methylpyridyl)porphyrins," *J. Phys. Chem.* **99**(13), 4397–4405 (1995).
32. G. De Luca, A. Romeo, and L. M. Scolaro, "Role of counteranions in acid-induced aggregation of isomeric tetrapyridylporphyrins in organic solvents," *J. Phys. Chem. B* **109**(15), 7149–7158 (2005).
33. M. A. J. Rodgers and P. T. Snowden, "Lifetime of O-2(1delta-G) in liquid water as determined by time-resolved infrared luminescence measurements," *J. Am. Chem. Soc.* **104**(20), 5541–5543 (1982).
34. S. Y. Egorov et al., "Rise and decay kinetics of photosensitized singlet oxygen luminescence in water—Measurements with nanosecond time-correlated single photon-counting technique," *Chem. Phys. Lett.* **163**(4–5), 421–424 (1989).
35. W. Baumler et al., "The role of singlet oxygen and oxygen concentration in photodynamic inactivation of bacteria," in *Proc. Natl. Acad. Sci. U. S. A.* **104**(17), 7223–7228 (2007).
36. J. R. Kanofsky et al., "Biochemical requirements for singlet oxygen production by purified human myeloperoxidase," *J. Clin. Invest.* **74**(4), 1489–1495 (1984).
37. D. N. Butorina, A. A. Krasnovskii, and A. V. Priezzhev, "Investigation of the kinetic parameters of singlet molecular oxygen in aqueous porphyrin solutions. influence of detergent and the quencher sodium azide," *Biofizika* **48**(2), 201–209 (2003).
38. J. M. Wessels, P. Charlesworth, and M. A. Rodgers, "Singlet oxygen luminescence spectra: a comparison of interferometer- and grating-based spectrometers," *Photochem. Photobiol.* **61**(4), 350–352 (1995).
39. S. Mitra et al., "Effective photosensitization and selectivity in vivo of Candida Albicans by meso-tetra (N-methyl-4-pyridyl) porphine tetra tosylate," *Lasers Surg. Med.* **43**(4), 324–332 (2011).
40. T. Ito, "Photodynamic action of hematoporphyrin on yeast cells–a kinetic approach," *Photochem. Photobiol.* **34**(4), 521–524 (1981).
41. M. P. Cormick et al., "Mechanistic insight of the photodynamic effect induced by tri- and tetra-cationic porphyrins on Candida albicans cells," *Photochem. Photobiol. Sci.* **10**(10), 1556–1561 (2011).
42. M. P. Cormick et al., "Photodynamic inactivation of Candida albicans sensitized by tri- and tetra-cationic porphyrin derivatives," *Eur. J. Med. Chem.* **44**(4), 1592–1599 (2009).
43. S. Oriel and Y. Nitzan, "Mechanistic aspects of photoinactivation of Candida albicans by exogenous porphyrins (dagger)," *Photochem. Photobiol.* **88**(3), 604–612 (2012).
44. R. F. Pasternack et al., "A spectroscopic and thermodynamic study of porphyrin/DNA supramolecular assemblies," *Biophys. J.* **75**(2), 1024–1031 (1998).
45. P. Kubat et al., "Interaction of novel cationic meso-tetraphenylporphyrins in the ground and excited states with DNA and nucleotides," *J. Chem. Soc.-Perkin Trans. 1*, **6**, 933–941 (2000).
46. P. Lopez-Chicon et al., "On the mechanism of Candida spp. photoinactivation by hypericin," *Photochem. Photobiol. Sci.* **11**(6), 1099–1107 (2012).
47. A. Eichner et al., "Dirty hands: photodynamic killing of human pathogens like EHEC, MRSA and Candida within seconds," *Photochem. Photobiol. Sci.* **12**(1), 135–147 (2012).